Geology, structural evolution, and hydrothermal alteration of the Island gold deposit, Michipicoten greenstone belt, Ontario

Tyler J. Ciufo[1*], Katia Jellicoe[1†], Chris Yakymchuk[1], Shoufa Lin[1], Patrick Mercier-Langevin[2], and Natasha Wodicka[3]

[1]University of Waterloo, 200 University Avenue West, Waterloo, Ontario N2L 3G1
[2]Geological Survey of Canada, 490 rue de la Couronne, Québec, Quebec G1K 9A9
[3]Geological Survey of Canada, 601 Booth Street, Ottawa, Ontario K1A 0E8
[*]Corresponding author's e-mail: tjciufo@uwaterloo.ca
[†]Corresponding author's e-mail: k.jellicoe@gmail.com

ABSTRACT

The Archean Island Gold deposit is situated in the Michipicoten greenstone belt within the Abitibi-Wawa subprovince. Gold mineralization is hosted in dacitic volcanic and volcaniclastic rocks, gabbro, and a tonalite-trondhjemite body (Webb Lake stock) within the southern domain of the east-west-trending Goudreau Lake deformation zone. The area is highly prospective, however, the controls on high-grade mineralization and the timing of events in the Michipicoten belt remain to be firmly established and compared with major gold systems of the southern Abitibi belt.

Several phases of deformation have affected the host rocks. The first deformation (D_1) event produced regional-scale folds. The second deformation (D_2) event resulted in camp-scale folds (F_2), a steep axial planar foliation (S_2), regional greenschist-grade metamorphism, and the formation of the Goudreau Lake deformation zone. The third deformation (D_3) event is expressed by brittle reverse faults, camp- to outcrop-scale folds (F_3), and a weakly developed axial planar (S_3) cleavage.

Gold mineralization in the main Island Gold ore zones was emplaced along the Goudreau Lake deformation zone during the D_2 deformation event. The Goudreau Lake deformation zone is inferred to be the major conduit that focused the gold-bearing fluids. The main ore zones dip steeply towards the south and consist of shear-hosted laminated quartz veins (V_1) and associated extensional veinlets (V_2). This V_1-V_2 veining is sub-parallel to the S_2 foliation and concentrated in the strain shadow of the pre-mineralization Webb Lake stock during D_2 north-side-up, sinistral transpression. Shallowly dipping, extensional quartz veins (V_{GD}) also host economic gold mineralization in the Goudreau Zone, which is located north of the main zones. The V_{GD} and V_1-V_2 veins are cut by extensional quartz veins (V_3) that formed during the third deformation (D_3) event in areas of high competency contrast. Post-mineralization tourmaline-quartz veins (V_4) locally overprint the V_3 veins and pre-existing structures.

Alteration envelopes associated with auriferous veining at the Island Gold deposit range from the centimetre to metre scale and are enriched in Au, K_2O, Rb, S, and Te, and depleted in Na_2O. Alteration minerals associated with ore zones generally include biotite, Ca-Mg-Fe carbonates, chlorite, plagioclase, quartz, sulphides (pyrite±pyrrhotite±chalcopyrite), and white mica (muscovite±phengite). Weak alteration associated with the late V_3 non-auriferous veins is variable and local.

The upper and lower absolute limits on the timing of gold mineralization are constrained by the U-Pb zircon ages of the mineralized Webb Lake stock (2724.1 ± 4.3 Ma) and the post-mineralization silica-poor diorite-monzodiorite (I2M) dykes (2672.2 ± 3.5 Ma). The youngest detrital zircon ages from overlying Doré sedimentary rocks, which were affected by syn-D_2 greenschist-facies metamorphism, further constrain the maximum age limit for the timing of gold mineralization to 2680 ± 3 Ma. This timing (2680 ± 3 Ma to 2672.2 ± 3.5 Ma) falls within the typical age range for gold deposits in greenstone belts of the Superior Province.

INTRODUCTION

Island Gold is an operating underground gold mine located approximately 35 km north of Wawa, Ontario, near the town of Dubreuilville. At the end of 2016, indicated and measured resources were estimated at 0.48 Mt at 5.94 g/t Au (91,400 oz) with inferred resources estimated at 3.04 Mt at 10.18 g/t Au (995,700 oz: Adam et al., 2017). Additionally, proven and probable mineral reserves were estimated at 2.55 Mt at 9.17 g/t Au (752,200 oz: Adam et al., 2017).

The Island Gold deposit is part of the Wawa gold camp, which is located between the major mining

Ciufo, T.J., Jellicoe, K., Yakymchuk, C., Lin, S., Mercier-Langevin, P., and Wodicka, N., 2020. Geology, structural evolution, and hydrothermal alteration of the Island Gold deposit, Michipicoten greenstone belt, Ontario; *in* Targeted Geoscience Initiative 5: Contributions to the Understanding of Canadian Gold Systems, (ed.) P. Mercier-Langevin, C.J.M. Lawley, and S. Castonguay; Geological Survey of Canada, Open File 8712, p. 143–156. https://doi.org/10.4095/323671

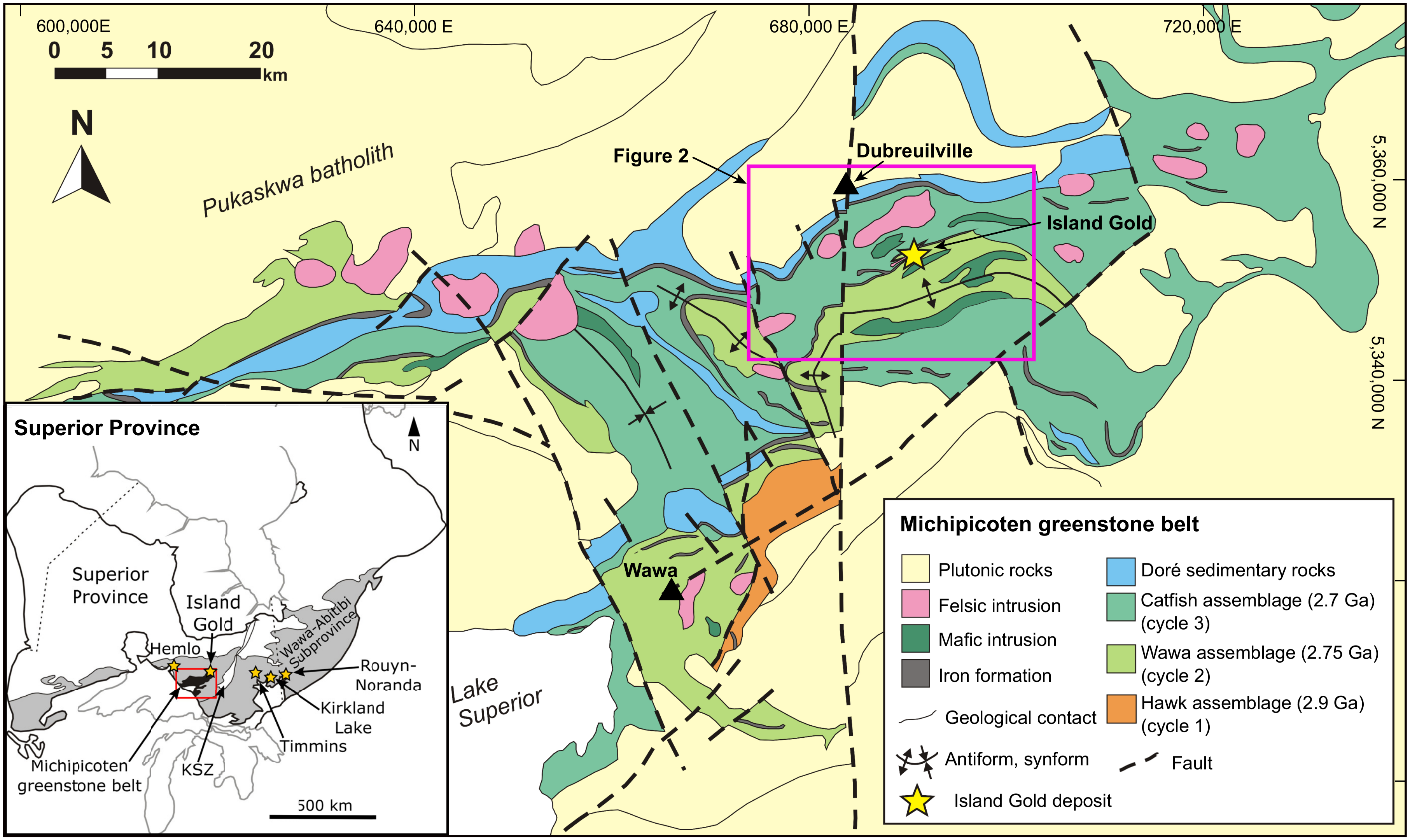

Figure 1. Geological map of the Michipicoten greenstone belt (*modified from* Arias and Heather, 1987; Williams et al., 1991; Jellicoe, 2019). The extent of Figure 2 is outlined by the purple rectangle. The inset delineates the location of the Michipicoten greenstone belt within the Abitibi-Wawa subprovince (*modified from* Card, 1990; Williams et al., 1991; Jellicoe, 2019). Abbreviation: KSZ = Kapuskasing structural zone.

camps of the Abitibi greenstone belt to the east (e.g. Kirkland Lake, Timmins, Val-d'Or, and Rouyn-Noranda), and the Hemlo gold camp to the west (Fig. 1). The deposit is hosted in the Goudreau Lake deformation zone (GLDZ), which has been compared with the gold-rich fault systems (specifically the Larder-Cadillac fault zone) that host numerous mining camps east of the Kapuskasing structural zone (Leclair et al., 1993; Fig. 1). The Wawa gold camp has not been as extensively studied as some of the other gold camps of the Abitibi-Wawa subprovince. The last study that included a detailed examination of the Island Gold deposit (Heather and Arias, 1992) predates the development of the Island Gold mine. Access to underground workings and drill core at Island Gold and in the vicinity allows access to a wealth of new information and data. This provides an opportunity to revisit the geology and metallogeny of a "re-emerging" district. Comparing the Island Gold deposit with other Archean gold deposits of the Abitibi greenstone belt will contribute to refining models for gold exploration in Archean terranes.

Two complementary M.Sc. research projects that focus on the structural and hydrothermal history of the Island Gold deposit commenced under the Gold Project of the Targeted Geoscience Initiative 5. The main findings of these projects are summarized here. Readers are referred to Jellicoe (2019) for detailed information about the deformation history, structural controls on ore, and the constraints on the timing of events, and to Ciufo (2019) for detailed information about the host lithologies, the nature and effects of hydrothermal alteration and metamorphism, and exploration vectors.

REGIONAL AND LOCAL GEOLOGY

The Island Gold deposit is located west of the Kapuskasing structural zone within the Abitibi-Wawa subprovince (Fig. 1). This subprovince consists mainly of east-west-trending supracrustal belts enveloped by larger granitoid-dominated areas. The volcanic and plutonic rocks mainly range in age from approximately 2.9 to 2.7 Ga and 2.9 to 2.6 Ga, respectively (Percival et al., 2012). The Michipicoten greenstone belt is located in the western part of the subprovince and hosts the Island Gold deposit. The Michipicoten greenstone belt is dominated by volcanic rocks that have been subdivided into three volcanic cycles: the ca. 2900 Ma Hawk assemblage, the ca. 2750 Ma Wawa assemblage, and the ca. 2700 Ma Catfish assemblage (Williams et al., 1991; Sage, 1994; Fig. 1). Each cycle has a mafic base and becomes more felsic towards the top. The first and second cycles are capped by unconformities separating the volcanic rocks from overlying iron formations. The volcanic and sedimentary rocks are cut by dioritic-gabbroic intrusions as well as granitic stocks of various ages (Sage et al., 1996). The Doré sedimentary rocks consist mainly of wacke and conglomerate that unconformably overlie the youngest volcanic cycle. The Doré sedimentary rocks are interpreted to be derived from the underlying volcanic rocks and their intrusive equivalents (Sage, 1994). Most rocks within the belt have been metamorphosed to greenschist facies, although contact aureoles of granitoid rocks at the outer margins of the belt can reach amphibolite grade (Rice and Donaldson, 1992). The granitoids proximal to the Michipicoten greenstone belt yield U-Pb ages mostly younger than, or equivalent to, the 2750 Ma Wawa cycle (Turek et al., 1982).

The Island Gold deposit is hosted by the GLDZ (Fig. 2) in the Goudreau-Lochalsh gold district of the Wawa gold camp. This 4.5 km wide regional structure is composed of multiple shear zones separating less strained domains. It has been traced along strike for >25 km (Arias and Heather, 1987). The Island Gold deposit is located in the southern domain of the GLDZ on the northern limb of the Goudreau anticline (Fig. 2). The southern domain is ~2 km wide, strikes N070°, and has been traced for ~8 km along strike (Arias and Heather, 1987). The Island Gold deposit is hosted mainly within the second cycle felsic-intermediate volcanic rocks of the Wawa assemblage (Arias and Helmstaedt, 1990) and, to a lesser extent, in mafic intrusive rocks (Fig. 3). The Michipicoten iron formation locally separates the cycle 2 felsic-intermediate volcanic rocks from the third cycle mafic volcanic rocks to the north. The Webb Lake stock, which hosts the Magino deposit a few kilometres west of the Island Gold mine (Fig. 3), forms an elongated intrusive body within the GLDZ. The Herman Lake nepheline-syenite intrusive complex (2671 +17/-10 Ma: Corfu and Sage, 1992) and the Maskinonge Lake granodiorite stock (2671 ± 2 Ma: Corfu and Sage, 1992) are large intrusive bodies located north of Island Gold (Fig. 2). Various pre- and post-ore dykes are also present in the Island Gold area.

HOST ROCKS, DEFORMATION, MINERALIZATION, AND ALTERATION

Field Relationships and Petrology

The main rock types present at the Island Gold mine include Wawa assemblage felsic-intermediate volcanic rocks, the Michipicoten iron formation, pre-ore mafic sills and dykes, the Webb Lake stock, and four sets of post-ore dykes (gabbro/lamprophyre, quartz diorite, I2M silica-poor diorite-monzodiorite, and diabase-quartz diabase). A summary of field relationships and petrological results is presented in this section for each of these lithologies. For more details, including methods and data, readers are referred to Ciufo (2019), Ciufo et al. (2019), and Jellicoe (2019).

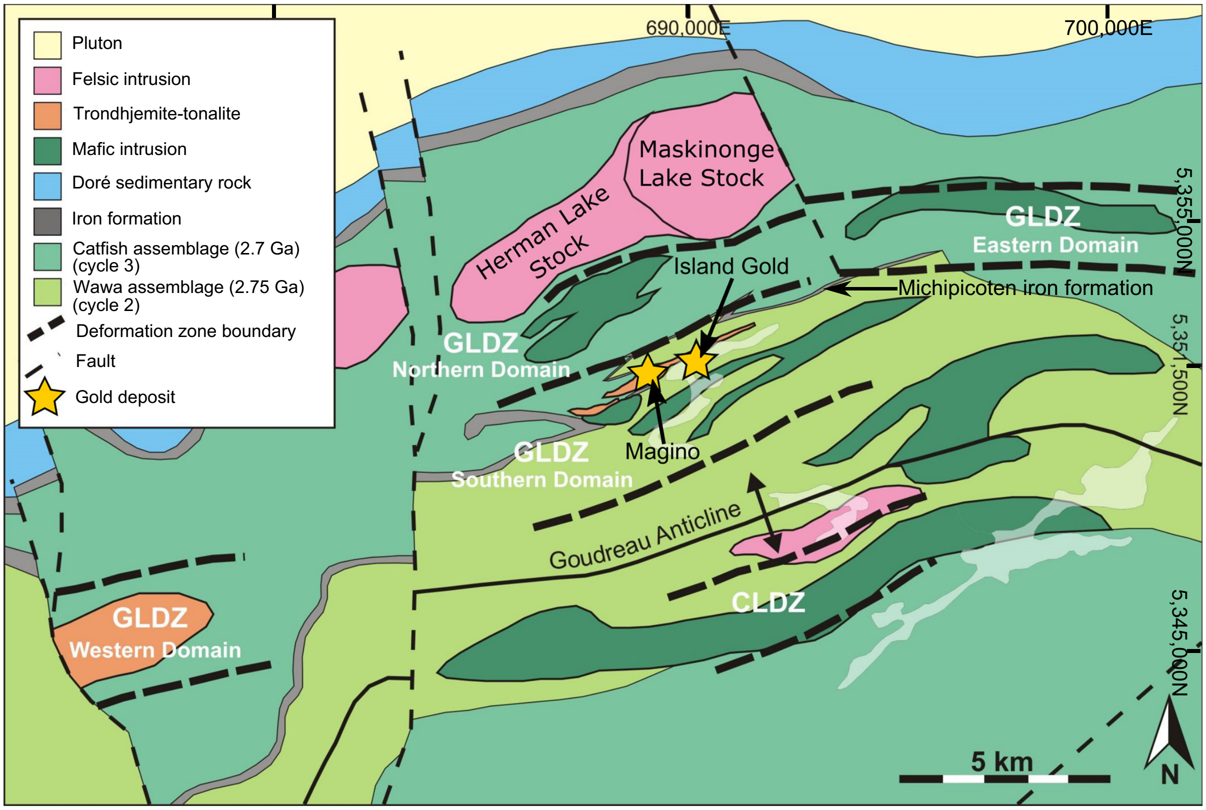

Figure 2. Geology of the Island Gold deposit and surrounding area (*modified from* Arias and Heather, 1987; Williams et al., 1991; and Jellicoe, 2019). Abbreviations: CLDZ = Cradle Lake deformation zone; GLDZ = Goudreau Lake deformation zone.

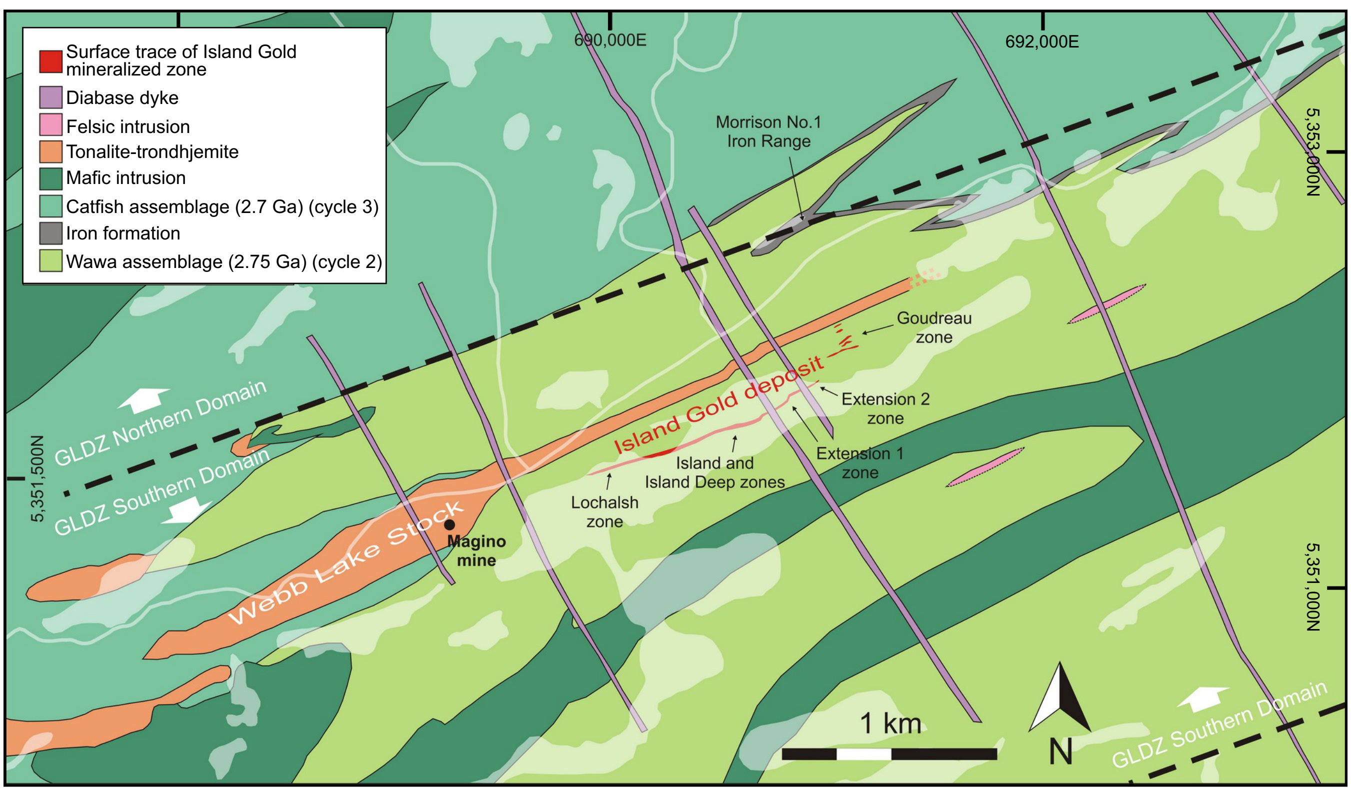

Figure 3. Geological map of the study area showing the southern Goudreau Lake deformation zone boundaries and the Island Gold deposit zones. Note the location of the Island Gold deposit relative to the Webb Lake stock. Partially transparent areas represent water bodies. *Modified from* Jellicoe (2019 and references therein).

The felsic-intermediate volcanic rocks (cycle 2, Wawa assemblage) are the most volumetrically significant lithologies at the Island Gold deposit (Fig. 3). They are also the oldest as they are stratigraphically overlain or crosscut by all other lithologies. They consist of tuff, lapilli tuff, tuff breccia, flows, and compositionally equivalent hypabyssal intrusive units. These rocks consist of plagioclase (andesine), quartz, calcite, biotite, chlorite, white mica (muscovite and illite), and epidote. Accessory minerals (typically <1 vol.%) include actinolite, apatite, chloritoid, grunerite, hematite, hornblende, ilmenite, magnetite, rutile, siderite, titanite, tourmaline, and zircon. These rocks are dacitic in composition (Ciufo, 2019), fine-grained (<1 mm), and often contain quartz and plagioclase phenocrysts (2–5 mm).

The Michipicoten iron formation stratigraphically overlies the dacitic volcanic rocks (Sage, 1994; Fig. 3), but thin iron formation beds are locally interlayered with the dacitic rocks as well. Sulphide and iron oxide-rich Algoma-type iron formation (cf. Gross, 1980) that can be massive or banded are present. Where banded, layers are composed of iron oxides (magnetite and hematite) and sulphides (mostly pyrite) alternating with chert, carbonate, and chlorite-rich layers. Accessory minerals include chloritoid, epidote, ilmenite, white mica, and tourmaline.

The pre-gold mineralization mafic intrusive rocks consist of gabbroic sills and dykes (Ciufo, 2019) and are cut by the auriferous veins in the ore zones. Their mineralogy consists of chlorite, quartz, epidote, carbonates (mostly calcite), actinolite, titanite, plagioclase (oligoclase–andesine), and hornblende. Accessory minerals include chloritoid, hematite, ilmenite, magnetite, clinopyroxene, rutile, tourmaline, and white mica (phengite). Most of the primary minerals in this lithology have been replaced with greenschist-facies minerals.

The Webb Lake stock is a relatively minor lithology at the Island Gold deposit, but it hosts the bulk of the ore at the Magino deposit to the west (Turcotte and Pelletier, 2008; Fig. 3). It is equigranular, medium- to coarse-grained, and intrudes the dacitic volcanic rocks, iron formation, and gabbro, and therefore post-dates these lithologies. It is composed of plagioclase (albite–oligoclase), quartz, chlorite, biotite, white mica (phengite±muscovite), epidote, and calcite. Accessory minerals include actinolite, apatite, chloritoid, hematite, hornblende, ilmenite, pyrite, pyroxene, rutile, titanite, tourmaline, and zircon. The Webb Lake stock is mainly tonalite with >10 vol.% ferromagnesian minerals (cf. Barker, 1979) but also has less abundant trondhjemitic phases composed of <10 vol.% ferromagnesian minerals (Ciufo, 2019).

Two distinct post-gold mineralization dyke sets commonly parallel and locally cut the V_1-V_2 ore zones (*see below* for vein nomenclature). One set consists of gabbro/lamprophyre composed of quartzo-feldspathic minerals (oligoclase-andesine and quartz), carbonate minerals, chlorite, and white mica. Accessory minerals include actinolite, epidote, hematite, rutile, titanite, tourmaline, and zircon. The other set consists of silica-poor diorite–monzodiorite (referred to as I2M by mine geologists), which is composed of plagioclase (oligoclase), carbonate minerals, biotite, chlorite, epidote, magnetite, and orthoclase. Accessory minerals include hematite, pyrite, quartz, rutile, titanite, tourmaline, white mica, and zircon. The silica-poor diorite-monzodiorite appears less deformed and metamorphosed than the gabbro/lamprophyre and therefore could be younger, although no clear crosscutting relationship between these two sets of dykes was observed. A minor quartz diorite dyke was exposed in one locality in the mine and as xenoliths within the silica-poor diorite-monzodiorite.

The lithologies discussed above in this section contain metamorphic assemblages that commonly include chlorite, actinolite, and epidote indicative of greenschist-facies metamorphism. Late diabase–quartz diabase dykes sharply cut all other lithologies and quartz veins, and are likely part of the Proterozoic Matachewan dyke swarm (Fig. 3).

Structural Geology

Three major deformation events (D_1 to D_3) affected the host rocks of the Island Gold deposit and surrounding rocks. The regional deformation event (D_1) is responsible for steepening of the volcanic and sedimentary rocks during regional- to camp-scale, northeast-southwest-striking upright folding (F_1) and formation of an axial-plane cleavage (S_1). The Goudreau anticline, the axial trace of which is located approximately two kilometres to the southeast of the Island Gold mine, is a regional F_1 fold (Fig. 2). The deposit is located on its northern limb in spatial association with a second-order parasitic synclinal fold to the Goudreau Anticline (Fig. 3). The Webb Lake stock tonalite-trondhjemite forms an elongate body along the axial plane of this parasitic fold, suggesting pre- or syn-D_1 deformation emplacement (Fig. 4).

The D_2 deformation event is a sinistral, north-side-up transpressional event. The GLDZ and associated S_2 foliation and L_2 stretching lineation formed during this event. Within the study area, the GLDZ strikes N070° with a gently sigmoidal trend (Heather and Arias, 1987) and follows the contact between the Wawa and Catfish assemblages (Fig. 3). The S_2 foliation is a penetrative foliation oriented subparallel to the strike of the GLDZ. It is expressed as schistosity in the volcanic rocks and the Webb Lake stock and displays a sinistral C-S fabric as well as sinistral offsets of veins along the

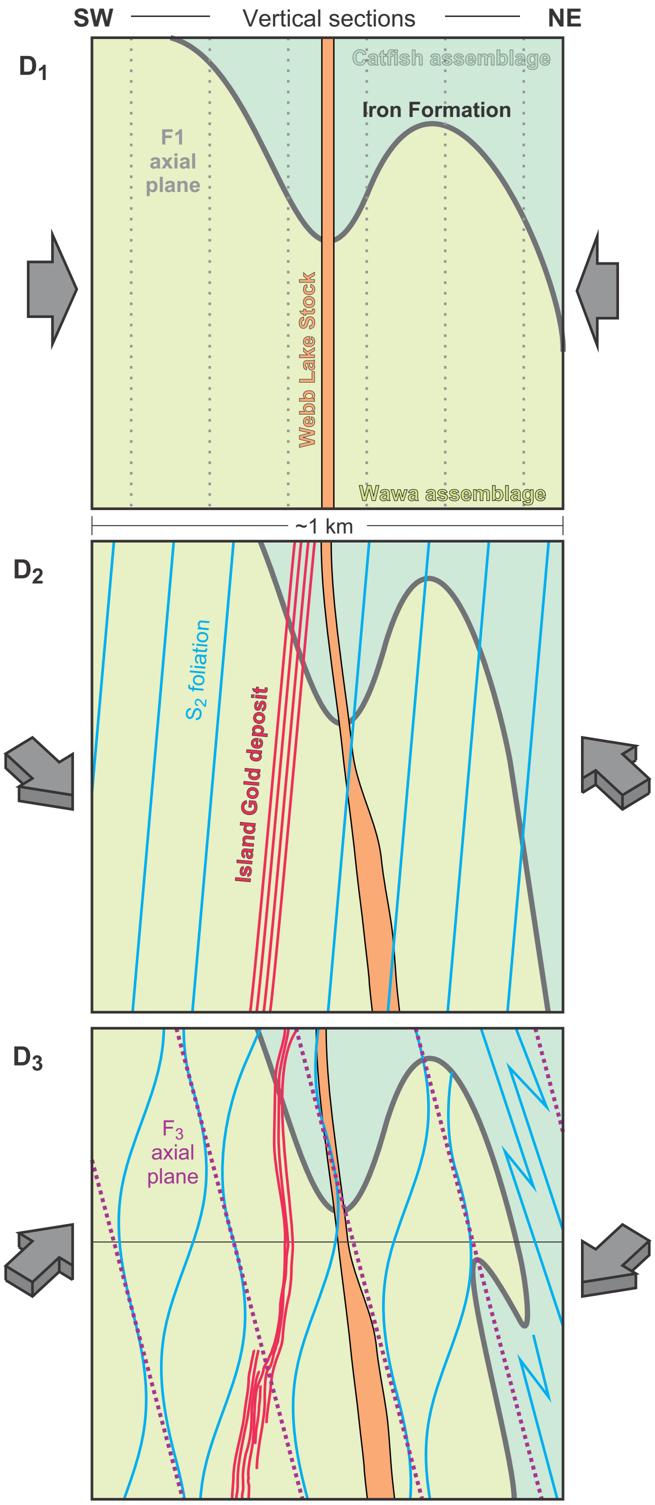

Figure 4. Schematic diagram showing the development of structures during $D_{1\text{-}3}$ deformation in the study area. Grey arrows represent principal shortening axes during progressive $D_{1\text{-}3}$ deformation. The horizontal grey line in the lowest block represents the current surficial expression.

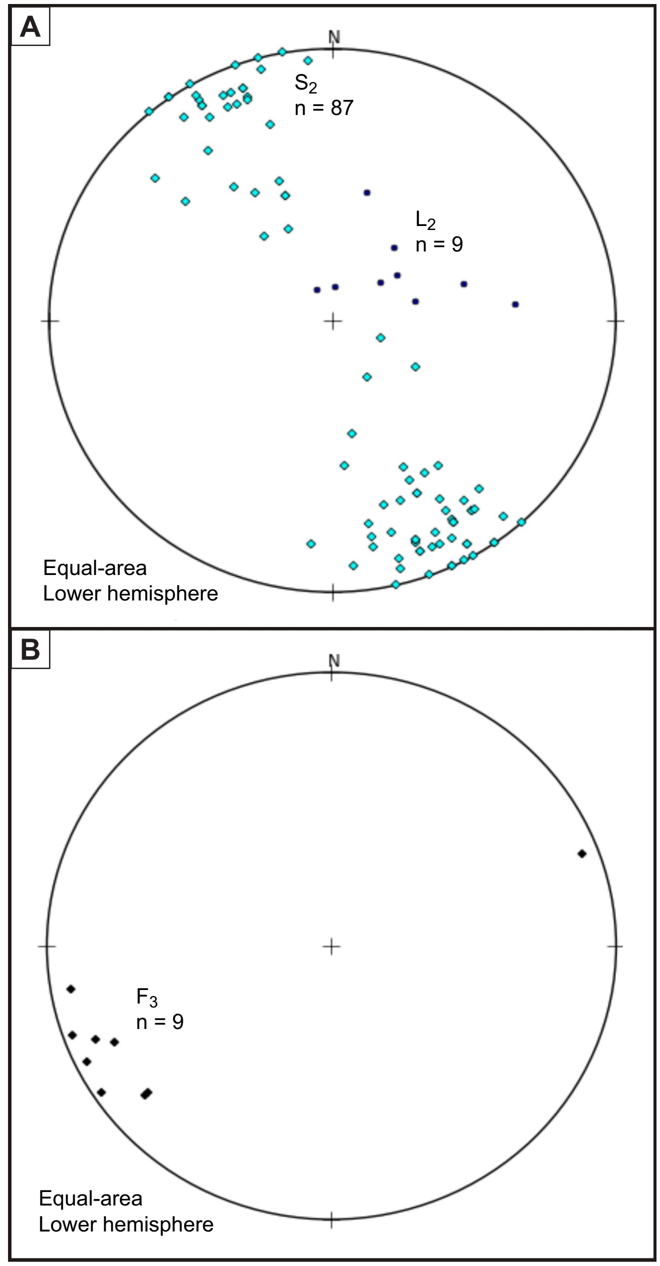

Figure 5. Stereographic projections: lower hemisphere equal area plots. **a)** Orientations of D_2 deformation fabrics in the study area. The light blue diamonds represent poles to S_2 foliation planes. The dark blue dots represent L_2 stretching lineations. **b)** Orientations of F_3 fold hinges (black diamonds) in the study area.

shear planes. The strike of the S_2 foliation is typically N070°, but ranges from N040° to N085°, with dips that vary from subhorizontal to subvertical (Fig. 5a). The L_2 stretching lineation, defined by stretched quartz and feldspar phenocrysts, plunges shallowly to steeply to the east along the S_2 foliation in the dacitic tuff. (Fig. 5a).

The D_3 deformation event produced camp- and outcrop-scale F_3 folds, an associated axial planar S_3 cleavage, and top-to-northwest reverse faults. The F_3 folds are open to tight, shallowly plunging, and Z-shaped. They occur at outcrop scale where they fold and transpose dykes and the S_2 foliation within the volcanic rocks and the Webb Lake stock, and at camp-scale

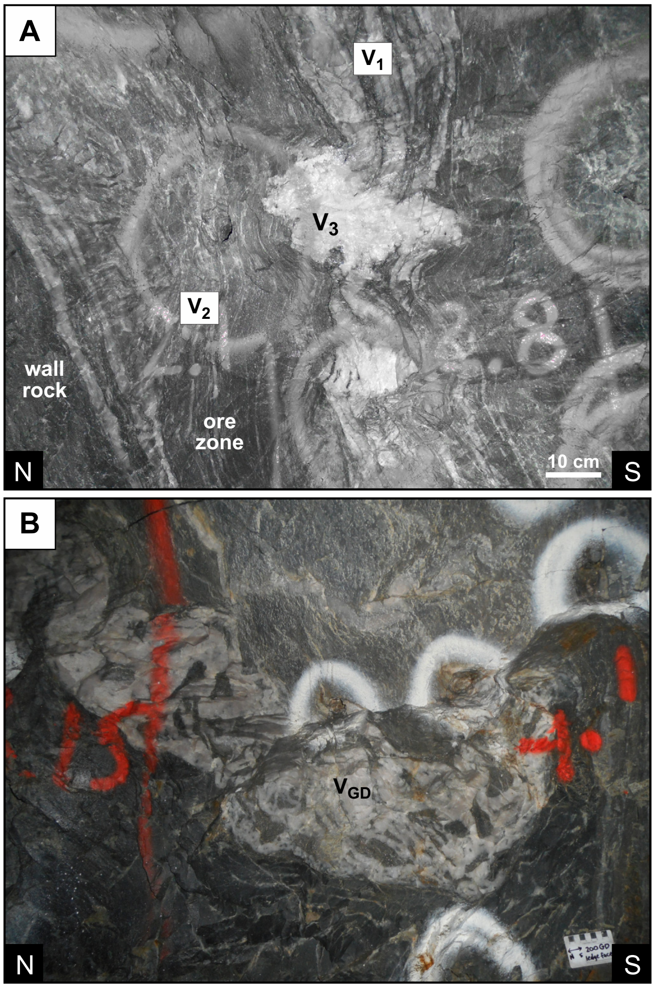

Figure 6. Photographs of vein sets found in the study area. **a)** An example showing the crosscutting relationships between V_1, V_2, and V_3 veins in the main Island zones. **b)** A typical example of a V_{GD} vein in the Goudreau Zone.

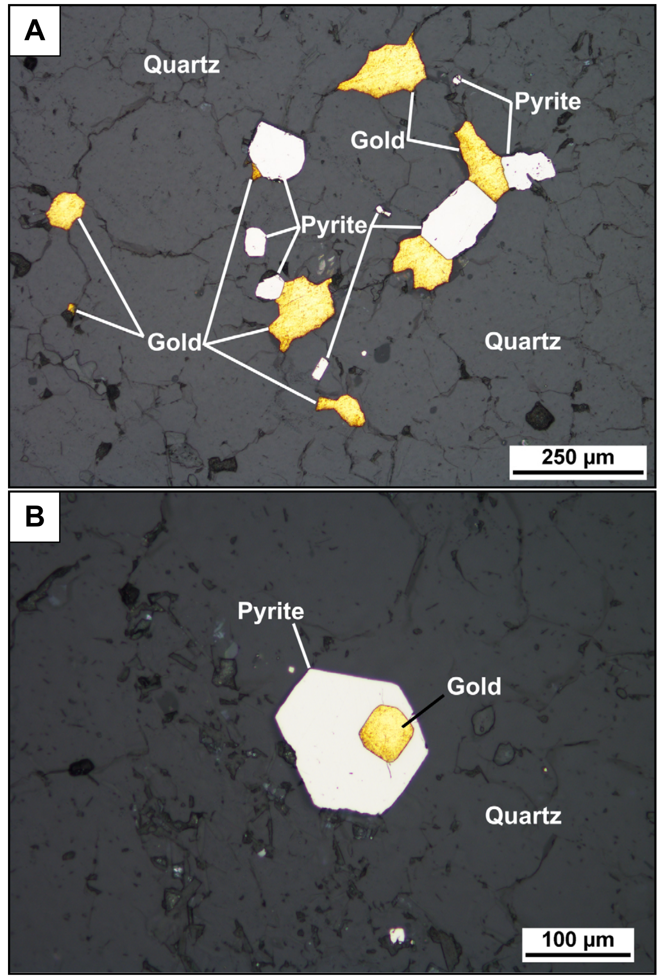

Figure 7. Reflected light photomicrographs of gold and sulphide minerals in quartz veins. **a)** Sulphides associated with gold. **b)** Gold inclusion in pyrite.

where they fold lithological contacts and the orebody. The poles to S_2 foliation form a girdle (Fig. 5a) that is sympathetic to F_3 fold axes (Fig. 5b), indicating that the variation in S_2 orientations is due to D_3 overprinting. The steeply north-dipping S_3 axial planar cleavage overprints the S_2 foliation and is weakly to moderately developed within folded felsic intrusions. In the northern part of the study area, the S_2 foliation is typically north-dipping and transposed subparallel to the S_3 axial planar cleavage.

Late brittle fractures, with minor (<1 m) offsets, overprint all previous structures. At the Island Gold deposit, mineralized zones (Extension 1 and 2 zones) show apparent sinistral offset of tens of metres along two diabase dykes, suggesting that the dykes were emplaced along brittle faults.

Vein Types and Gold Mineralization

Two types of veins are present in most of the ore zones throughout the Island Gold deposit: V_1 shear veins and V_2 extensional veins (Fig. 6a). Mutually crosscutting relationships and their close spatial association with each other suggest that the V_1 and V_2 veins (V_1-V_2) formed during the same gold mineralizing event. They also have overlapping alteration envelopes. White-coloured, semi-translucent, extensional quartz veins are present in the Goudreau Zone (V_{GD} veins) and these veins are folded and shallowly plunging (Fig. 6b). A shear zone hosting V_1-V_2 veins was observed offsetting a V_{GD} vein suggesting that V_1-V_2 veining postdates V_{GD} veining. The V_{GD}, V_1, and V_2 veins often crosscut and alter the dacite, gabbro, and Webb Lake stock, and commonly contain macroscopically visible gold. Envelopes of alteration progressively increase in intensity towards these veins, and although gold is present in these alteration envelopes, the highest concentrations are found within the veins.

Most of the gold within V_{GD}, V_1, and V_2 veins occurs as free gold along mineral grain boundaries in the form of micrometre- to millimetre-scale laminations, veinlets, or irregular masses (Fig. 7a). Occasionally, gold is present as inclusions within other

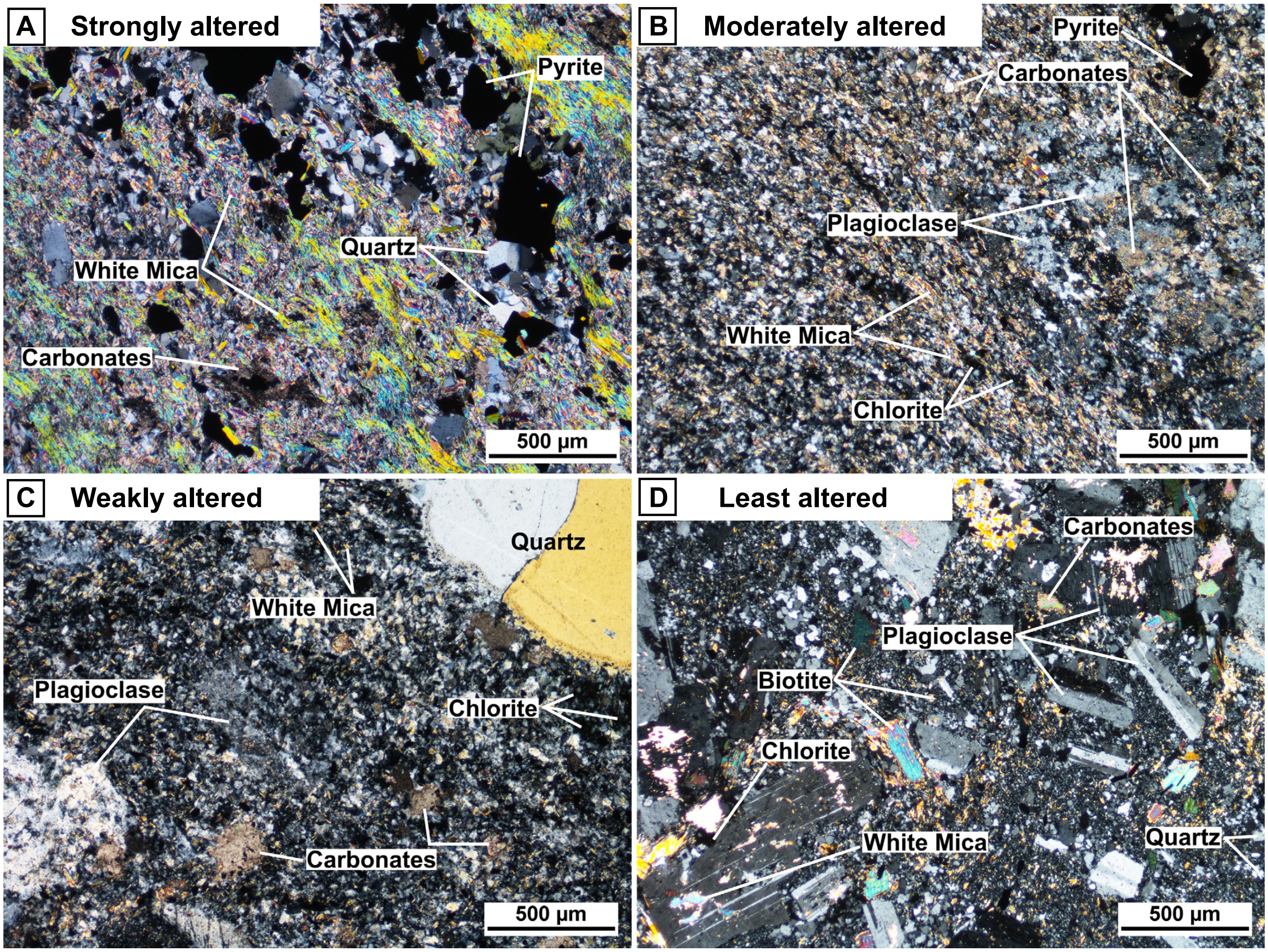

Figure 8. Cross-polarized transmitted light photomicrographs of dacitic samples that are variably altered by V_1-V_2 veins. The amount of pyrite, quartz, and white mica increase with increases alteration intensity. The proportions of plagioclase and primary biotite decrease with increasing alteration.

minerals such as quartz, carbonate, white mica, and pyrite grains (Fig. 7b). In all cases, gold is spatially associated with sulphide minerals within a few hundred micrometres. Less commonly, gold grains are present within the altered V_{GD}, V_1, and V_2 vein selvages. Gold grains in V_{GD}, V_1, and V_2 veins may also contain minor silver (<15 wt%).

A fourth vein-type (V_3) consists of barren, quartz-carbonate extensional veins that cut across all lithologies, with the exception of the diabase–quartz diabase, and also frequently cut across ore zones (Fig. 6a). Typically, V_{GD}, V_1, V_2, and V_3 quartz veins are composed of >90 % quartz and <10% carbonate minerals (calcite±dolomite±ankerite).

Tourmaline may be present as semi-planar ribbons (V_4 veins) or disseminated within various lithologies as well as within V_{GD}, V_1, V_2, and V_3 quartz veins. The tourmaline ribbons are commonly parallel to these veins, as well as various other contact surfaces. In addition to tourmaline, V_4 veins occasionally contain minor quartz and carbonate minerals. Tourmaline occurs within and postdates all lithologies and vein types, with the exception of the diabase-quartz diabase dykes.

Alteration and Vectors for Gold Mineralization

Isocon diagrams and mass balance calculations were used to determine consistent chemical mass gains and losses due to alteration based on the whole-rock geochemistry of multiple altered and less-altered sample pairs. Alteration strength groupings were initially outlined based on proximity to auriferous quartz veins and qualitative estimates of alteration intensity and later quantified on the basis of K_2O and S concentration. The methods used to determine immobile chemical species are outlined in Ciufo (2019). Alteration related to V_1-V_2 veining at the Island Gold deposit (e.g. Fig. 8a–d, 9) resulted in the enrichment of Au, K_2O, Rb, S, and Te, and typically depletion in Na_2O in alteration envelopes developed in dacite, gabbro, and the Webb

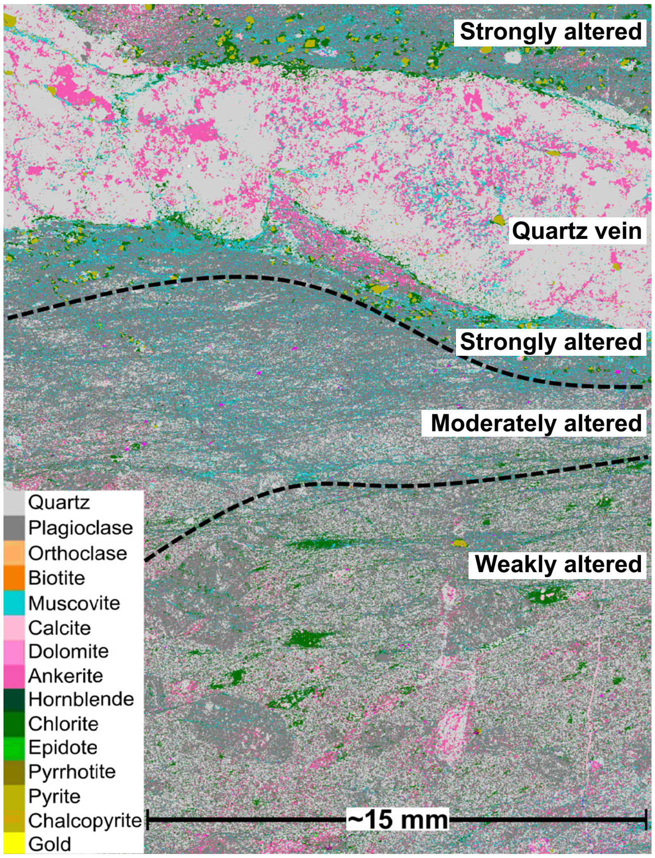

Figure 9. Scanning electron microscope mineral liberation analysis (SEM-MLA) image (using false colours to depict different minerals) of a V_2 quartz veinlet and an associated miniature dacite-hosted alteration envelope in a thin section. Approximate boundaries between alteration strength groupings are displayed.

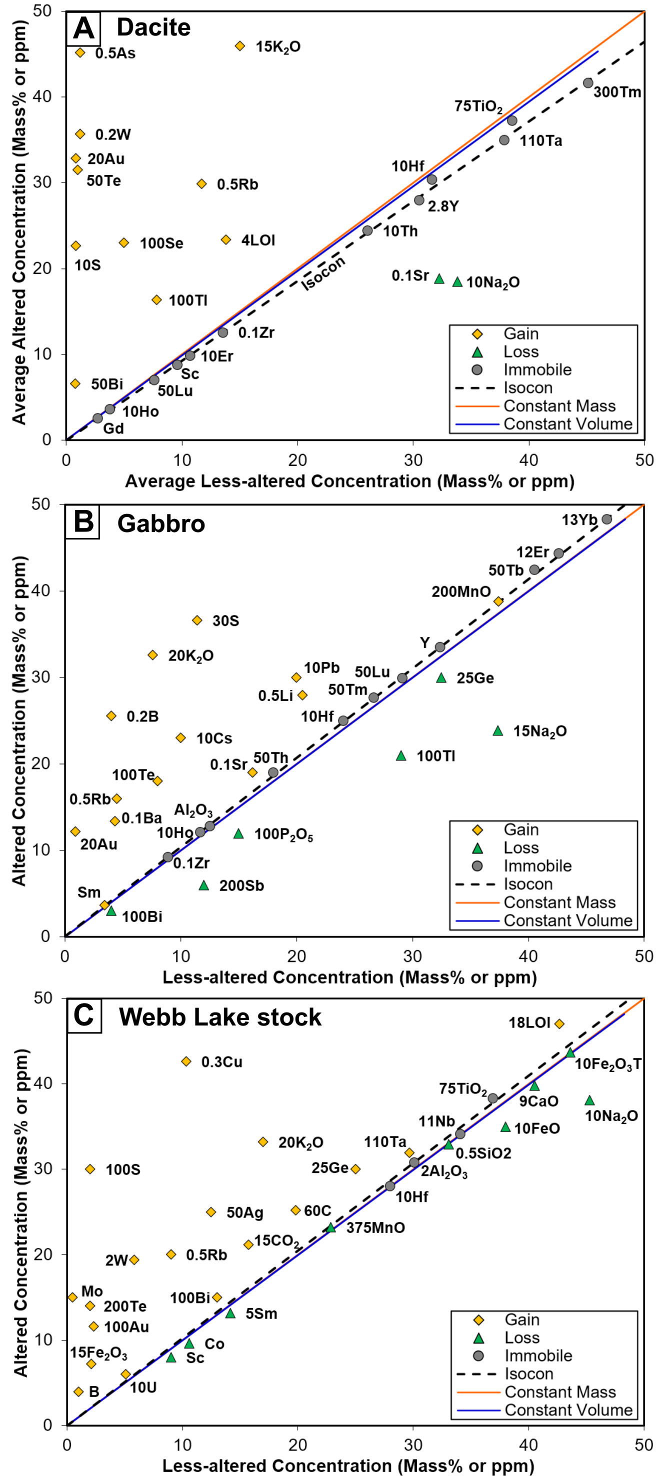

Figure 10. Isocon diagrams displaying the composition of samples of **(a)** dacite, **(b)** gabbro, and **(c)** the Webb Lake stock altered by V_1-V_2 veins plotted against the composition of corresponding less altered samples. In addition to relatively immobile chemical species, only chemical species that are consistently enriched or depleted due to alteration of that lithology are displayed. Concentrations of elements are arbitrarily scaled to avoid stacking/overlap and scale factors are displayed in front of each chemical species. Abbreviations: Fe_2O_3T= total iron; LOI= loss on ignition. Methodology details are given in Ciufo (2019).

Lake stock. Other common enrichments include As, Se, and W. Other consistent chemical gains and losses specific to dacite, gabbro, and the Webb Lake stock due to auriferous alteration are summarized in Figure 10.

Alteration minerals associated with V_1-V_2 auriferous quartz veining mainly consist of biotite, Ca-Mg-Fe carbonates, chlorite, plagioclase, quartz, sulphides (pyrite±pyrrhotite±chalcopyrite), and white mica (muscovite±phengite; e.g. Fig. 8a–c, 9). Changes in mineral proportions from strongly altered to least altered rock are depicted in Figure 11 for each of the three main host lithologies. The alteration mineral assemblage and mineral proportions vary depending on the host rock. In all lithologies, the volumetric proportion of potassic micas (sum of biotite and white mica) and sulphide minerals generally increases with increasing alteration intensity (Fig. 11). Based on the study of multiple alteration envelopes associated with V_1-V_2 veining at various locations throughout the deposit, the alteration minerals and major chemical gains remain relatively consistent. The mineralogical and chemical signature of alteration related to V_{GD} veins in the dacite is similar to that of alteration related to V_1-V_2

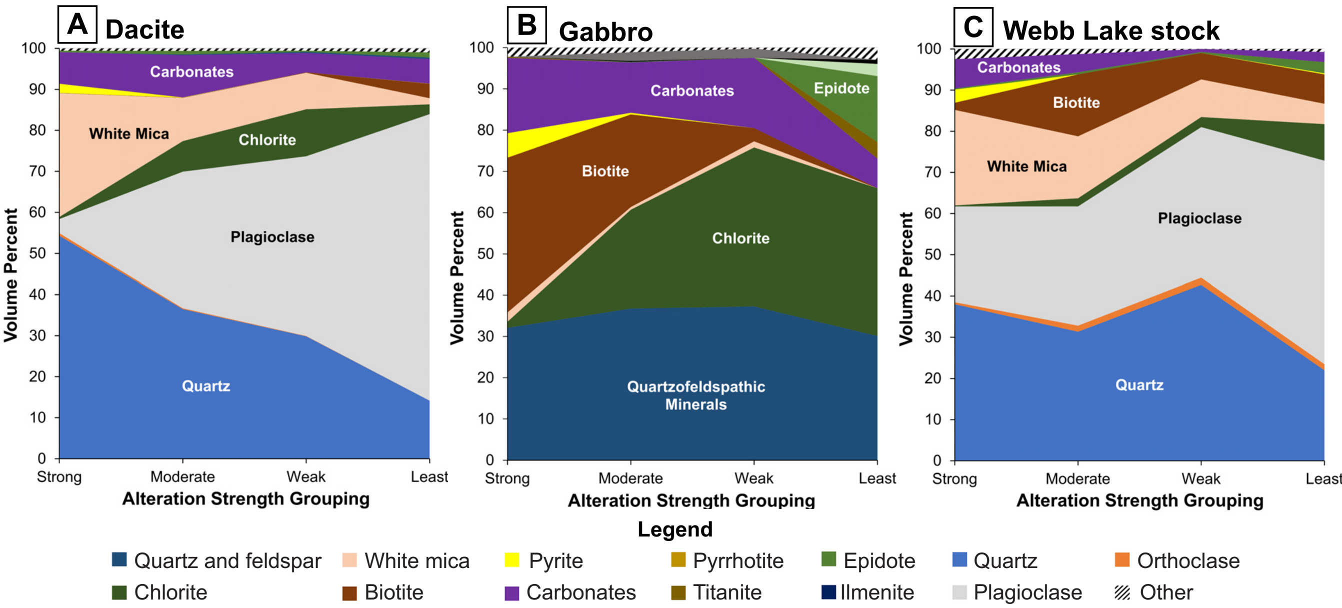

Figure 11. Mineral proportions in samples of **(a)** dacite, **(b)** gabbro, and **(c)** the Webb Lake stock variably altered by auriferous V_1-V_2 quartz veins. Mineral proportions were determined via scanning electron microscope mineral liberation analysis (SEM-MLA) for dacite and point-counting was used for gabbro and the Webb Lake stock.

veins in the same lithology (Ciufo, 2019). One side of an alteration envelope associated with auriferous quartz veining (V_1-V_2 and V_{GD}) can range in thickness from a few centimetres to 10 m or more perpendicularly outwards from a central vein to the outer margin of the alteration envelope.

The V_1, V_2, and V_{GD} quartz veins and their associated diffuse zones of silicification ("quartz flooding") are the most reliable indicators for gold grades that are >4 g/t at the Island Gold deposit. In low-grade samples (1–4 g/t Au), pyrite mode correlates well with gold grade. Samples with greater than 3 vol.% sulphide minerals (pyrite±pyrrhotite±chalcopyrite) typically have grades of >1 g/t Au. Proportions of alteration minerals, such as biotite, carbonates, chlorite, quartz, sericite, and sulphides, can be used as an approximate guide to determine the intensity of alteration (Fig. 11). Subsequently, this can be used to help estimate gold grade as gold concentrations that are >1 g/t are typically found in either strongly altered rock or auriferous quartz veins (Fig. 12). Increased proportions of chlorite and carbonate minerals relative to unaltered rock can be used to identify the weakly altered outer margins of alteration envelopes associated with auriferous quartz veins.

The V_3 veins have either no associated visible alteration or have local envelopes of weak alteration that typically do not extend more than 20 cm from the vein/wall-rock contact. Chemical mass gains and losses are minor, inconsistent, and vary depending on the host rock in which the veins formed (Ciufo, 2019).

Tourmalinization (V_4 veins) was probably unrelated to the main gold mineralizing events as least altered

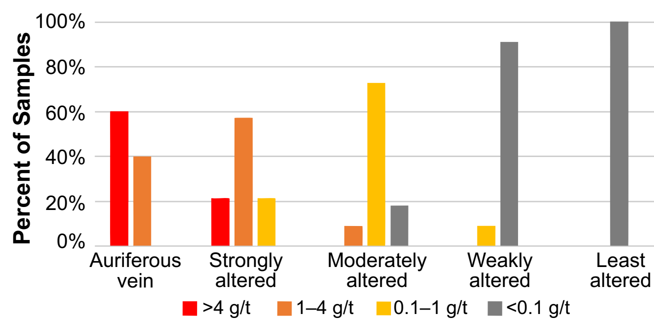

Figure 12. Samples of dacite, gabbro, the Webb Lake stock, as well as V_{GD} and V_1-V_2 auriferous quartz veins, are subdivided into five groupings: auriferous vein, strongly altered, moderately altered, weakly altered, and least altered (Ciufo, 2019). This histogram displays the proportion of these samples within each of the five groupings that fall into each of the gold-grade intervals outlined in the legend.

samples often contain tourmaline. Additionally, these least altered tourmaline-bearing samples have low gold grades, which are equivalent to least altered samples that are absent of tourmaline. In many cases, the tourmaline ribbons/veins have no visible alteration envelope.

U–Pb Zircon Geochronology

To better constrain the timing of events at the Island Gold deposit, two samples were analyzed for U-Pb zircon geochronology using a sensitive high-resolution ion microprobe. The zircons were analyzed at the J.C. Roddick Ion Microprobe Laboratory at the Geological Survey of Canada. Readers are referred to Jellicoe (2019) for analytical procedures and detailed results. Sample SH-3 is a drill core sample from a drillhole that intersected mineralized tonalite-trondhjemite of the

Webb Lake stock at a depth of 550 m below surface. Zircons from this sample yield a preliminary weighted mean $^{207}Pb/^{206}Pb$ age of 2724.1 ± 4.3 Ma (n = 23/24; mean square weighted deviation (MSWD = 1.5), which is inferred to be the crystallization age of the Webb Lake stock. It also provides a maximum age for gold mineralization (as discussed below).

Sample KJM095 is from a barren, silica-poor diorite-monzodiorite intrusion (I2M) that cuts across the Island ore zones at depth. The sample was collected from the 740 metre level underground workings of the Island Gold mine. The absence of pervasive fabric or alteration in the dyke suggests that it was emplaced late- or post-D_2 shearing and regional greenschist-grade metamorphism. The zircon grains from sample KJM095 define a preliminary weighted mean $^{207}Pb/^{206}Pb$ age of 2672.2 ± 3.5 Ma (n = 24/24, MSWD = 1.2), which is interpreted as the crystallization age of the silica-poor diorite-monzodiorite, and the minimum age for gold mineralization.

DISCUSSION

Structural History and Age of Gold Mineralization

The emplacement of the Webb Lake stock along an F_1 fold axial surface occurred before or during D_1 deformation. The Webb Lake stock acted as a more competent body during D_2 deformation. A large protrusion along the southwest edge of the Webb Lake stock (Fig. 3) passively created a strain shadow to the southeast. Dilation along the edge of this strain shadow allowed emplacement of V_1 and V_2 veins along the S_2 foliation, forming a mineralized corridor (Fig. 13). During D_3 deformation, the F_3 folds overprinted the S_2 foliation and the V_1 and V_2 veins, and the V_3 veins were emplaced in shallowly dipping extensional fractures (Fig. 4). The V_{GD} veins in the Goudreau Zone appear to be distinct from the V_1-V_2 veins of the main Island and Extension zones. V_{GD} veins are believed to represent an earlier, separate mineralizing event. Further investigation into the controls on this mineralizing event and its timing relative to the Island and Extension zones is necessary to confirm how the Goudreau Zone fits into the overall genetic model of the Island Gold deposit. Although the D_2-related V_1 shear veins and associated V_2 extensional veins represent the main mineralized features, hydrothermal activity in the area might have been protracted, or more than one mineralizing event may have affected the Island Gold deposit; this has potential implications for exploration at the camp scale.

U-Pb zircon ages from the mineralized Webb Lake stock (2724.1 ± 4.3 Ma) and the I2M post-mineralization dyke (2672.2 ± 3.5 Ma) define absolute constraints

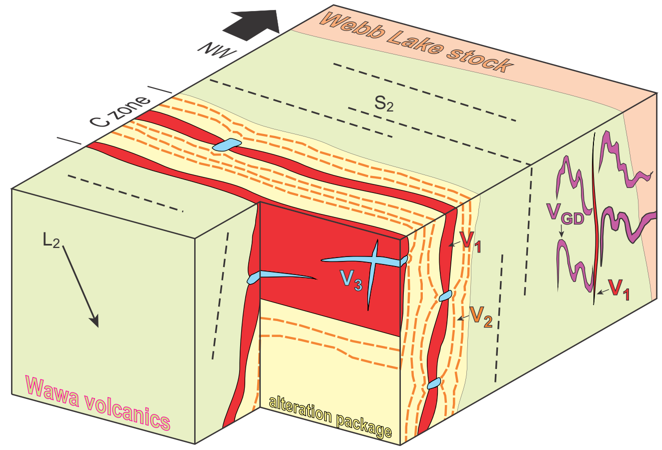

Figure 13. Schematic block diagram showing the geometry of D_2 deformation fabrics and the vein sets of the Island Gold deposit. The C zone is one of the main ore zones at the Island Gold deposit. Not to scale.

on the timing of gold mineralization at the Island Gold deposit. Like the Webb Lake stock and I2M, the overlying Doré sedimentary rocks were also affected by greenschist-facies metamorphism and the age of the youngest analyzed detrital zircon is 2680 ± 3 Ma (Corfu and Sage, 1992). D_2 deformation occurred during regional greenschist-facies metamorphism indicating that D_2 deformation began shortly after the deposition and subsequent rapid burial of the Doré sediments, and further constrains the timing of mineralization to post-2680 ± 3 Ma.

The likely age range for gold mineralization at the Island Gold deposit (between 2680 ± 3 Ma and 2672.2 ± 3.5 Ma) is consistent with the age of gold mineralization at the Hemlo deposit to the west (ca. 2677 Ma: Davis and Lin, 2003) that also took place during D_2 deformation (Lin, 2001) and during extensive ca. 2686–2677 Ma sanukitoid magmatism (Lin and Beakhouse, 2013 and references therein). Robert et al. (2005) and Dubé and Gosselin (2007) suggest that the peak of orogenic gold mineralization (greenstone-hosted quartz-carbonate vein systems) in the southern Abitibi greenstone belt occurred syn- to late-main deformation and late- to post-peak greenschist-facies metamorphism (i.e. <2670 Ma, the maximum age of the Timiskaming orogenic conglomerate, and postdates ca. 2680–2670 Ma alkaline magmatism±volcanism). However, there are post-volcanic, structurally controlled gold deposits that are slightly older in the Abitibi (e.g. the Kiena mine, which has a minimum age of gold mineralization of 2686 Ma: Morasse et al., 1995). More recently, Lin and Beakhouse (2013) suggested that gold mineralization, Timiskaming-type sedimentation and sanukitoid/alkaline magmatism were generally synchronous and probably related to the same tectonic process (synchronous vertical and horizontal tectonism) at the late stage of Archean cratonization. In any case, the timing of gold mineralization at Island Gold falls within the age range of peak gold mineralization in the southern Abitibi greenstone belt. However, gold mineralization at Island Gold is perhaps slightly older than, or coeval with, the alkaline magmatism in the area based on the available U-Pb ages. More work is necessary to decipher the precise timing relationships between sedimentation, calc-alkaline to alkaline magmatism, and gold deposition at camp scale.

Although the GLDZ represents a major D_2 deformation corridor, it is not clear if it represents a first-order structure. Its nature, location in the district, and direct spatial association with gold suggest that it is perhaps rather a second- or third-order structure. If that is the case, it then raises the question about the location of what could be a first-order structure, or precursor major fault in the district, which is of crucial importance to understand gold metallogenesis and improve exploration models in the district.

Auriferous Alteration

Alteration associated with gold mineralization at the Island Gold deposit is similar to other orogenic gold deposits, including the presence of biotite, carbonates, chlorite, plagioclase, sericite, and sulphides in the auriferous alteration assemblage. Similar geochemical features include enrichments in As, Au, K, S, Te, and W in areas proximal to auriferous quartz veining (Groves et al., 1998).

The GLDZ, which hosts the Island Gold deposit, has been correlated with the large fault systems east of the Kapuskasing structural zone that host major orogenic gold deposits (Leclair et al., 1993). Studies of some of these gold deposits near Kirkland Lake (e.g. Kerr-Addison, Young-Davidson, Beattie), Rouyn-Noranda (e.g. Francoeur 3), and Timmins (e.g. Hoyle Pond, Dome) (Fig. 1) show similar geochemical alteration haloes. These deposits are typically characterized by enrichments in Au, K_2O, Rb, and S (Kishida and Kerrich, 1987; Moritz and Crocket, 1991; Couture and Pilote, 1993; Dinel et al., 2008; Bigot, 2012; Martin, 2012), which is consistent with the Island Gold deposit. Other common enrichments in these gold deposits east of the Kapuskasing structural zone include As, Ba, CO_2 (and/or volatiles/LOI), SiO_2, and W. These enrichments are also developed in auriferous vein-related alteration at the Island Gold deposit but do not consistently occur for all altered/less-altered pairs and each host lithology. In orogenic gold deposits east of the Kapuskasing structural zone, Na enrichment in the wall rock around auriferous quartz veins is common (e.g. Kishida and Kerrich, 1987; Couture and Pilote, 1993; Dinel et al., 2008; Martin, 2012). However, Na depletion occurs at the Island Gold deposit and also in some deposits east of the Kapuskasing structural zone, such as at the Beattie Gold deposit (Bigot, 2012).

In deposits that are located east of the Kapuskasing structural zone in the Abitibi-Wawa subprovince, gold-related alteration minerals typically include carbonate minerals, chlorite, sericite, and/or potassium feldspar, plagioclase, quartz, and sulphide minerals (Kishida and Kerrich, 1987; Smith et al., 1987; Moritz and Crocket, 1991; Couture and Pilote, 1993; Dinel et al., 2008; Bigot, 2012; Martin, 2012). Although biotite is not typically an alteration mineral at these deposits, it is an alteration mineral present in gabbro and in Webb Lake stock-hosted ore zones at the Island Gold deposit. In addition, although present in minor quantities, potassium feldspar is not a major alteration mineral in any lithologies at Island Gold. Similar to deposits east of the Kapuskasing structural zone, carbonate minerals, chlorite, sericite, plagioclase, quartz, and sulphides are all significant alteration minerals at the Island Gold deposit.

The overall consistency of the auriferous alteration at Island Gold deposit relative to these other deposits east of the Kapuskasing structural zone suggests a similar genetic history. However, the chemical and mineralogical footprint of gold-related hydrothermal alteration at each of these deposits is not identical. This is probably due to differences in the nature of host rocks, with Island Gold deposit being predominantly hosted in intermediate to felsic volcanic rocks, whereas many major orogenic gold deposits are hosted in mafic volcanic and sedimentary rocks, and in some cases, alkaline intrusions. This indicates that, although similar, both the composition of the auriferous fluids and the associated alteration mineral assemblages vary between deposits in response to local conditions.

IMPLICATIONS FOR EXPLORATION AND MINING

The results of this study provide improved guidelines for exploration. For example, exploration within the GLDZ should prioritize areas of high competency contrast within shear zones (e.g. intrusions and lithological contacts). The “lee-side” of intrusive bodies at the time of D_2 deformation should represent areas of particular interest as the Webb Lake stock acted more competently than the surrounding volcanic rocks in the GLDZ, thereby creating a strain shadow in which fluid circulation was facilitated and auriferous quartz veins preferentially formed. This exploration strategy can also be applied to other prospective deformation zones elsewhere.

The thorough documentation and classification of the types of auriferous veins and associated alteration envelopes will aid in identifying, tracking, and modelling the auriferous vein systems at the mine and in the surrounding area and standardize mapping and core logging. In particular, alteration mineral assemblages and geochemistry can be used to identify subtle alteration and vector towards areas with an increased potential for gold.

The main orebody is oriented subparallel to S_2 foliation and the plunge of the L_2 lineation. The ability to explain and better anticipate the geometry of the ore zones in this structurally controlled deposit will help improve ore zone correlation, production drillhole targeting, mine planning, and reconciliation.

ACKNOWLEDGMENTS

This report is a contribution to NRCan's Targeted Geoscience Initiative Program (TGI-5) Gold Project. Support for this study was provided through Activity G-1.1: Gold through space and time at the Archean. We thank Alamos Gold Inc. and Richmont Mines Inc. for logistical, scientific, and financial support. We acknowledge funding from the Natural Sciences and Engineering Research Council of Canada. In addition, we thank the staff at the Island Gold mine, J. Richardson, B. Kendall, and other staff and students at the University of Waterloo for their assistance and recommendations. The scanning electron microscope mineral liberation analysis (SEM-MLA) laboratory work was conducted by D. Grant, D. Goudie, and Memorial University staff at the CREAIT Network's Micro Analysis Facility SEM/MLA Lab. Electron microprobe laboratory analyses were conducted with the help of M. Beauchamp at the Earth and Planetary Material Analysis Laboratory at Western University. Zircon mineral separates were prepared by R. Chung and G. Case at the Geological Survey of Canada. P. Hunt oversaw zircon imaging for in-situ SHRIMP analyses. SHRIMP data acquisition and data reduction were conducted with the help of T. Pestaj and N. Rayner. We also express our gratitude to E. Ambrose and V. Bécu (technical editors), S. Castonguay (scientific editor), and B. Lafrance (external reviewer) for their insightful revisions. For a complete version of this summary of acknowledgements, readers are referred to Ciufo (2019) and Jellicoe (2019).

REFERENCES

Adam, D., LeBlanc, L.G., Bélisle, M., Ramcharan, V.K., and Vincent, R., 2017. Island Gold mine technical report and expansion case preliminary economic assessment, Dubreuilville, Ontario, Canada, Technical report according to National Instrument 43-101 and Form 43-101F1; Richmont Mines Inc. <https://www.sedar.com> [accessed February 1, 2020]

Arias, Z.G. and Heather, K.B., 1987. Regional structural geology related to gold mineralization in the Goudreau-Lochalsh area, District of Algoma; *in* Summary of Field Work and Other Activities; Ontario Geological Survey, Miscellaneous Paper 137, p. 146–154.

Arias, Z.G. and Helmstaedt, H., 1990. Grant 343-Structural evolution of the Michipicoten (Wawa) greenstone belt, Superior Province: Evidence for an Archean fold and thrust belt; *in* Geoscience Research Grant Program Summary of Research 1989–1990, (ed.) V.G. Milne; Ontario Geological Survey, Miscellaneous Paper 150, p. 107–114.

Barker, F., 1979. Trondhjemite: Definition, environment and hypotheses of origin; *in* Trondhjemites, Dacites, and Related Rocks, (ed.) F. Barker; Elsevier, Developments in Petrology, Amsterdam, Vol. 4, p. 1–12.

Bigot, L., 2012. Gold mineralizations at the syenite-hosted Beattie gold deposit at Duparquet, Neoarchean Abitibi belt, Quebec, Canada; M.Sc. thesis, Université du Québec à Montréal, Montréal, Quebec, 136 p.

Card, K.D., 1990. A review of the Superior Province of the Canadian Shield, a product of Archean accretion; Precambrian Research, v. 48, p. 99–156.

Ciufo, T.J., 2019. Hydrothermal alteration and exploration vectors at the Island Gold deposit, Michipicoten greenstone belt, Wawa, Ontario; M.Sc. thesis, University of Waterloo, Waterloo, Ontario, 510 p.

Ciufo, T., Mercier-Langevin, P., Yakymchuk, C., Lin, S., Bécu, V., and Lauzière, K., 2019. Whole-rock lithogeochemistry of the Archean Island Gold deposit Ontario, Canada; Geological Survey of Canada, Open File 8524, 1 .zip file.

Corfu, F. and Sage, R.P., 1992. U-Pb age constraints for the deposition of clastic metasedimentary rocks and late-tectonic plutonism, Michipicoten Belt, Superior Province; Canadian Journal of Earth Sciences, v. 29, p. 1640–1651.

Couture, J.-F. and Pilote, P., 1993. The geology and alteration patterns of a disseminated, shear zone-hosted mesothermal gold deposit: The Francoeur 3 deposit, Rouyn-Noranda, Quebec; Economic Geology, v. 88, p. 1664–1684.

Davis, D.W. and Lin, S., 2003. Unravelling the geologic history of the Hemlo Archean gold deposit, Superior Province, Canada: A U-Pb geochronological study; Economic Geology, v. 98, p. 51–67.

Dinel, E., Fowler, A.D., Ayer, J., Still, A., Tylee, K., and Barr, E., 2008. Lithogeochemical and stratigraphic controls on gold mineralization within the metavolcanic rocks of the Hoyle Pond mine, Timmins, Ontario; Economic Geology, v. 103, p. 1341–1363.

Dubé, B. and Gosselin, P., 2007. Greenstone-hosted quartz-carbonate vein deposits in Mineral Deposits of Canada – A Synthesis of Major-Types, District Metallogeny, the Evolution of Geological Provinces, and Exploration Methods, (ed.) W.D. Goodfellow; Geological Association of Canada, Mineral Deposits Division, Special Publication No. 5, p. 49–73.

Gross, G.A., 1980. A classification of iron formations based on depositional environments; The Canadian Mineralogist, v. 18, p. 215–222.

Groves, D.I., Goldfarb, R.J., Gebre-Mariam, M., Hagemann, S.G., and Robert, F., 1998. Orogenic gold deposits: A proposed classification in the context of their crustal distribution and relationship to other gold deposit types; Ore Geology Reviews, v. 13, p. 7–27.

Heather, K.B. and Arias, Z.G., 1987. 024: Geological setting of gold mineralization in the Goudreau-Lochalsh area, district of Algoma; *in* Summary of Field Work and Other Activities 1987, (ed.) R.B. Barlow, M.E. Cherry, A.C. Colvine, B.O. Dressler, and O.L. White; Ontario Geological Survey, Miscellaneous Paper 137, p. 155–162.

Heather, K.B. and Arias, Z., 1992. Geological and structural setting of gold mineralization in the Goudreau-Lochalsh area, Wawa gold camp; Ontario Geological Survey, Open File Report 5832, 159 p.

Jellicoe, K.M., 2019. Structural controls and deformation history of the orogenic Island Gold deposit, Michipicoten greenstone belt, Ontario; M.Sc. thesis, University of Waterloo, Waterloo, Ontario, 84 p.

Kishida, A. and Kerrich, R., 1987. Hydrothermal alteration zoning and gold concentration at the Kerr-Addison Archean lode gold deposit, Kirkland Lake, Ontario; Economic Geology, v. 82, p. 649–690.

Leclair, A.D., Ernst, R.E., and Hattori, K., 1993. Crustal-scale auriferous shear zones in the central Superior Province, Canada; Geology, v. 21, p. 399–402.

Lin, S., 2001. Stratigraphic and structural setting of the Hemlo gold deposit, Ontario, Canada; Economic Geology, v. 96, p. 477–507.

Lin, S. and Beakhouse, G.P., 2013. Synchronous vertical and horizontal tectonism at late stages of Archean cratonization and genesis of Hemlo gold deposit, Superior craton, Ontario; Geology, v. 41, p. 359–362.

Martin, R.D., 2012. Syenite-hosted gold mineralization and hydrothermal alteration at the Young-Davidson deposit, Matachewan, Ontario; M.Sc. thesis, University of Waterloo, Waterloo, Ontario, 172 p.

Morasse, S., Wasteneys, H., Cormier, M., Helmstaed, H., and Mason, R., 1995. A pre-2686 Ma intrusion-related gold deposit at the Kiena mine, Val d'Or, Quebec, southern Abitibi subprovince; Economic Geology v. 90, p. 1310–1321.

Moritz, R.P. and Crocket, J.H., 1991. Hydrothermal wall-rock alteration and the formation of the gold-bearing quartz-fuchsite vein at the Dome mine, Timmins area, Ontario, Canada; Economic Geology, v. 86, p. 620–643.

Percival, J.A., Skulski, T., Sanborn-Barrie, M., Stott, G.M., Leclair, A.D., Corkery, M.T., and Boily, M., 2012. Geology and tectonic evolution of the Superior Province, Canada; Chapter 6 *in* Tectonic Styles in Canada: The LITHOPROBE Perspective, (ed.) J.A. Percival, F.A. Cook, and R.M. Clowes; Geological Association of Canada, Special Paper 49, p. 321–378.

Rice, R.J. and Donaldson, J.A., 1992. Sedimentology of the Archean Doré metasediments, Arliss Lake area, southern Michipicoten greenstone belt, Superior Province; Canadian Journal of Earth Sciences, v. 29, p. 2558–2570.

Robert, F., Poulsen, H.K., Cassidy, K.F., and Hodgson, C.J., 2005. Gold metallogeny of the Superior and Yilgarn cratons; *in* Economic Geology 100th Anniversary Volume, (ed.) J.W. Hedenquist, J.F.H. Thompson, R.J. Goldfarb, and J.P. Richards; Society of Economic Geologists, p. 1001–1033.

Sage, R.P., 1994. Geology of the Michipicoten greenstone belt; Ontario Geological Survey, Open File Report 5888, 592 p.

Sage, R.P., Lightfoot, P.C., and Doherty, W., 1996. Geochemical characteristics of granitoid rocks from within the Archean Michipicoten greenstone belt, Wawa Subprovince, Superior Province, Canada: implications for source regions and tectonic evolution; Precambrian Research, v. 76, p. 155-190.

Smith, E.J., Kesler, S.E., and Van Hees, E.H.P., 1987. Relationship of fluid inclusion geochemistry to wall-rock alteration and lithogeochemical zonation at the Hollinger-McIntyre gold deposit, Porcupine district, Canada; Journal of Geochemical Exploration, v. 29, p. 434.

Turcotte, B. and Pelletier, C., 2008. Technical report and mineral resource estimate for the Magino mine (according to Regulation 43-101 and Form 43-101F1); InnovExplo for Golden Goose Resources Inc. <https://www.sedar.com> [accessed February 1, 2020]

Turek, A., Smith. P.E., and Van Schmus, W.R., 1982. Rb-Sr and U-Pb ages of volcanics and granite emplacement in the Michipicoten belt-Wawa, Ontario; Canadian Journal of Earth Sciences, v. 19, p. 1608–1626.

Williams, H.R., Scott, G.M., Heather, K.B., Muir, T.L., and Sage, R.P., 1991. Wawa Subprovince; Chapter 12 *in* Geology of Ontario, (ed.) P.C. Thurston, H.R. Williams, R.H. Sutcliffe, and G.M. Stott; Ontario Geological Survey, Special Volume 4, Part 1, p. 485–539.